Theory of Size Dependent Deliquescence of Nanoparticles: Relation to Heterogeneous Nucleation and Comparison with Experiments

ARTICLE *in* THE JOURNAL OF PHYSICAL CHEMISTRY B · JULY 2001

Impact Factor: 3.3 · DOI: 10.1021/jp010537e

Theory of Size Dependent Deliquescence of Nanoparticles: Relation to Heterogeneous Nucleation and Comparison with Experiments

Y. S. Djikaev,* R. Bowles, and H. Reiss

Department of Chemistry and Biochemistry, UCLA, Los Angeles, California 90095

K. Hämeri

Finnish Institute of Occupational Health, Laajaniityntie 1, FIN-01620 Vantaa, Finland

A. Laaksonen

Department of Applied Physics, University of Kuopio, P.O. Box 1627, FIN-70211 Kuopio, Finland

M. Väkevä

Department of Physics, University of Helsinki, P.O. Box 9, FIN-00014 Helsinki, Finland

Received: February 12, 2001; In Final Form: June 5, 2001

In this paper, we develop a thermodynamic theory for the deliquescence behavior of soluble crystals in an atmosphere of solvent vapor. In this endeavor, we have focused on studying possible free energy barriers that could impede deliquescence. Our aim was to construct a theory general enough to treat both macroscopic and nanosized crystals. Toward this end, as a first attempt, we focused on a theory capable of describing the qualitative features of the results of recent experimental measurements, especially in the nanometer range where interfacial effects are bound to play a role. However, we have also opted for simplicity, and with this in mind, the surface thermodynamics that we have used are of the simplest type, ignoring crystal shape, rigorously defined dividing surfaces, curvature dependence of surface tension, and the presence of surface excess (adsorption). We do however include the effects of "disjoining pressure". Nevertheless, we are able to describe several of the observed features and to calculate free energy surfaces traversed by the path of a deliquescing system. Analyses of these paths enable us to define two types of deliquescence, "nucleate" and "activate", that occur respectively with and without a free energy barrier. A most important experimental behavioral feature that the theory cannot yet comfortably describe is the apparent existence, for nanosized and micron sized crystals, of ranges of vapor saturation ratio within which there is a continuum of deliquescent states such that a film of solution coexists in equilibrium with the core crystal. Within our thermodynamic theory, such coexistence can only be achieved using draconian measures such as the choice of interfacial tensions that have an unphysical behavior. Because, in the case of micron sized crystals, surface effects cannot be responsible for the coexistence of core and film, this together with the difficulty encountered in fashioning a thermodynamic theory, incorporating surface phenomena, that allows such coexistence, suggests that apparent nonprompt deliquescence must be due to some other factor such as the state of the initial core crystals. The measurements on small crystals involved $(NH_4)_2SO_4-H_2O$ and $NaCl-H_2O$ systems and were performed using a tandem differential mobility analyzer. Aside from the failure to predict continuous deliquescence, our first results are promising, and a more sophisticated thermodynamic theory should provide a more thorough description of the observed features of deliquescence.

1. Problem Background

There is little doubt that the formation and growth of atmospheric cloud droplets occurs as a result of the condensation of water vapor and other atmospheric gases onto preexisting aerosols usually called "cloud condensation nuclei" (CCN). Some of the most important CCN are soluble particles of inorganic salts such as NaCl, $(NH_4)_2SO_4$, as well as mixed particles that consist partly of such compounds.

For clarity of presentation of the material that forms the focus of this paper, we will adopt a slight modification of terminology: CCN will be referred to as "particles" rather than "nuclei".

The initial stage of formation of a droplet on a soluble (or mixed soluble−insoluble) particle involves "deliquescence" during which the particle gradually dissolves so that a liquid film of aqueous solution forms around it. This composite structure may or may not become a condensation nucleus before the solid core (or at least its soluble component) is completely dissolved.

Since the pioneering work of Köhler,[1−3] many papers dealing with the condensation on hygroscopic aerosols have been published (for a short review, see refs 4 and 5). As a rule however, these authors were primarily concerned with the determination of the degree of supersaturation of water vapor such that condensation became barrierless, i.e., with the supersaturation at which the particle was activated in the Köhler sense,

* To whom correspondence should be addressed. E-mail: djikaev@chem.ucla.edu.

10.1021/jp010537e CCC: $20.00
Published on Web 07/17/2001

and only a few attempted to deal with the problem of partial dissolution of the particle. An example of the latter is furnished by the work of Kuni and co-workers, who assumed that, during the formation of the droplet, the film was in quasiequilibrium with the soluble core.[6,7] With this assumption, they were able to specify the critical supersaturation for barrierless condensation (activation) for the case of a core that was only partially dissolved.

None of the above authors investigated the influence of particle size on the process of deliquescence. However, recently, Mirabel, Reiss, and Bowles (MRB) published a thermodynamic theory[8,9] dealing with the deliquescence of a small particle and its dependence on size. In this work, surface thermodynamics was used in an effort to determine how the supersaturation required for the initiation of deliquescence depended on particle size. Because MRB were only interested in deriving the qualitative features of the phenomenon, the formulation of surface thermodynamics that they used was unsophisticated, e.g., it was of the sort that, in the field of nucleation, has come to be known as the "capillarity approximation".[10] In this approximation, an embryo for a phase transition is modeled as a small drop, crystal, or bubble having a uniform interior density and a sharp interface with a surrounding phase, to which a curvature independent surface tension (frequently that of a macroscopic entity) is assigned. This approach has probably had more success than it deserves, but it has been able to describe the qualitative features of many nucleation processes, and for this reason, MRB applied it to the deliquescence problem.

The deliquescence of large particles (micron size) has been studied experimentally and extensively by Tang and co-workers[11,12] using electrodynamic levitation. Besides, the deliquescence of submicrometer particles has been studied using a tandem differential mobility analyzer (TDMA) technique (see, e.g., ref 13). Tang and co-workers noticed that deliquescence was "prompt" at the deliquescence pressure; the soluble crystal (e.g., NaCl or $(NH_4)_2SO_4$) seemed to dissolve sharply and fully at a single critical pressure of water vapor (the deliquescence pressure), and thereafter, the drop of solution grew in accordance with nonideal Raoult's law as the relative humidity (RH) was increased. However, upon decreasing the RH, the system did not retrace the path followed with increasing RH. Instead, the drop of solution persisted below the deliquescence pressure until the RH was reduced to a critical value at which crystal nucleation within the drop occurred, accompanied by efflorescence. Such hysteresis was the general rule. However, the sharpness of the deliquescence moved MRB to assume that coexistence of solution and crystal did not occur, so that deliquescence did not involve an equality of chemical potentials of the two phases, crystal and solution, but rather took place when the free energies of the undeliquesced initial system, vapor and solid crystal, and the final system, vapor and drop of solution, were equal. In essence, this assumption implies that the transformation from solid to liquid is not impeded by a free energy barrier. On the basis of this assumption, a dependence of deliquescence pressure on crystal size was demonstrated. However, as we discuss below, it now seems evident that smaller soluble crystals (10−50 nm), and even some larger crystals, do not deliquesce promptly but rather over a range of supersaturations, although the amended theory in the present paper still predicts that small crystals will dissolve promptly.

As already indicated, there is now evidence[12,13c] that, in some circumstances, even micron-sized particles can deliquesce over a range of supersaturations. This implies that such "continuous" deliquescence does not have to be due to the effects of surface phenomena, because, in micron range, surface effects must be of negligible consequence. Then the cause of nonsharp deliquescence in the nanometer range need not be sought only in terms of interfacial of surface thermodynamics (though, clearly, surface phenomena can play here a significant role). As we shall see, only the most draconian steps in the modification of a theory based on surface thermodynamics has allowed us to predict an equilibrium coexistence of a soluble crystalline core and a film of encapsulating solution as would be required in an explanation of nonsharp deliquescence based on surface phenomena. Our calculations indicate that either there is still some surface thermodynamic feature missing from our theory or some bulk phenomenon takes place in the experiments that is difficult to account for. Experimental data[12,13c] indicate that the latter alternative seems to be the case with ammonium sulfate (note, however, that whether this holds in other systems remains an open question). Nonsharp deliquescence in these experiments could then conceivably be due to the physical or chemical state of the initial soluble particle, a state which may be difficult to fully characterize.

Does this mean that our theory is equivalent, fully, to the original MRB theory? The answer is "no" because in that theory it is assumed that the condition for barrierless deliquescence is the equality of the free energies of the undeliquesced and fully deliquesced systems. These systems represent the "reactant" and "product" states in the deliquescence "reaction", and at the disappearance of the barrier, these states need not have equal free energies. For example, the product state could have a lower free energy than the reactant state. The proper condition for the disappearance of the barrier is the equality of the free energies of the system in the reactant state and in the state at the top of the barrier (in which case there *is* no barrier). Consequently, in this paper, we examine the barrier with the goal of determining the level of vapor supersaturation at which it disappears. This involves some modification of the MRB equations, and so we cannot simply refer to the analytical development of their paper. Instead, the modified derivation presented in this paper is necessary.

One of the bases for considering "nonpromptness", or nonsharpness, is a unique series of experiments on the deliquescence of crystals in the nanometer range performed by Hämeri et al.[14] in a tandem differential mobility analyzer (TDMA) which was specially designed for nanometer sized particles. MRB had suggested such experiments[8,9] and in a remarkable example of serendipity, Hämeri et al.[14] independently performed them without ever having communicated with MRB whose paper had not yet appeared in the open literature. Figure 1, taken from Hämeri et al.,[14] shows some of their results.

It was the nonsharpness of the phenomenon that induced the present authors, now consisting of a collaboration between individuals from both the MRB and Hämeri groups, to undertake the present modification of the original MRB theory (although many of the equations are retained) in an effort to explain the qualitative features of the TDMA results. As already indicated, this modification, and the comparison of theory with experiment, as well as the examination of the relation to "nucleation", forms the basis of the present paper. An important new idea involves the introduction of "disjoining pressure"[15] into the theory. However, as in the earlier work,[8,9] the level of thermodynamics remains at the "capillarity approximation". For condensed systems (solid or liquid particles), this means that both the crystal and the solution are regarded as incompressible and that interfaces are sharp. Furthermore, we do not explicitly introduce Gibbs dividing surfaces or surfaces of tension,[16−19] and surface

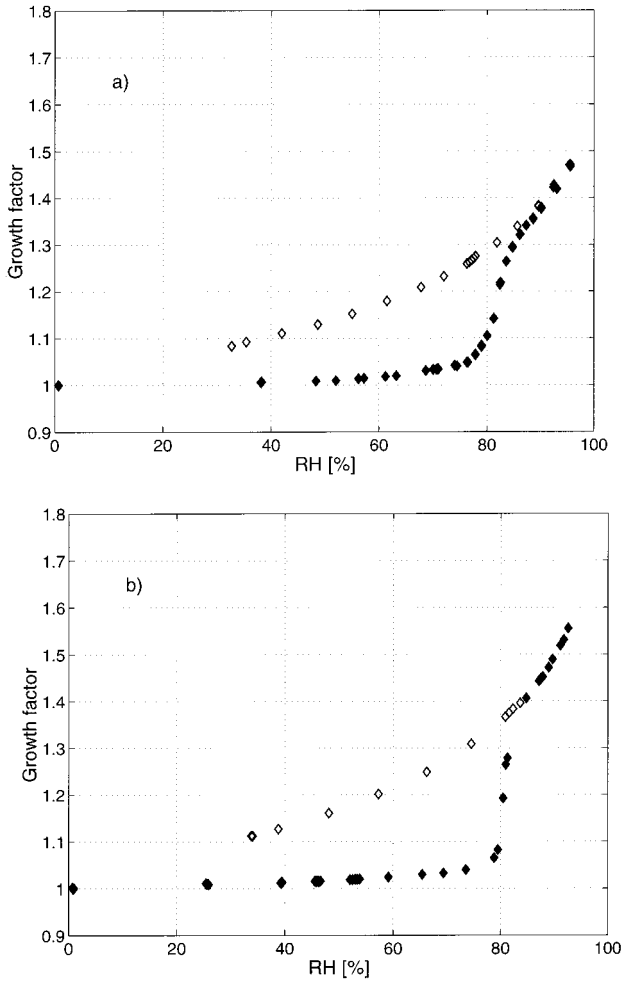

Figure 1. Growth factor, R/r_0, as a function of relative humidity, RH $= \zeta \times 100\%$, for $(NH_4)_2SO_4$ particles of dry radii: (a) $r_0 = 5$ nm and (b) $r_0 = 7.5$ nm. Data at increasing RH are indicated by solid black symbols, and data at decreasing RH are shown by open symbols.

tension is assumed to be independent of curvature. In addition, we assume that the components of the system are not surface active so that it is not necessary to consider surface adsorption.[16−19]

How far these assumptions cause the theory to depart from physical reality remains problematical, but in a later paper, we hope to present an analysis that begins with a more rigorous Gibbsian approach, gradually eliminating rigorous elements in favor of approximations that ultimately reduce the system to the level of the capillarity approximation. In this way, we hope to see the effect of each approximation, or alternatively, the approximations that are actually contained in the capillarity approximation.

In this connection, however, even before proceeding with the main development of the present paper, it is appropriate to reemphasize that we have found the theory (approximate at the capillarity level) to be almost incapable of fully reproducing the qualitative features of the experimental data of ref 14, or of additional data, beyond that for ammonium sulfate, now available for sodium chloride.[20] Figure 1 shows the absence of a "sharp" deliquescence that we have been unable to explain. The deliquescence, "continuous" as a function of RH, as exhibited by the data in the figure, could imply a stable equilibrium, characterized by coexistence between a liquid film of solution and a solid core that it encapsulates. However, as has already been mentioned, new data on micron sized particles suggest that the reason for this behavior lies elsewhere. Also,

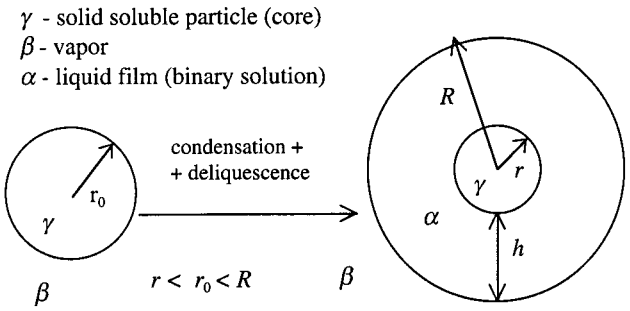

Figure 2. Scheme of droplet formation on a soluble particle of initial radius r_0. The droplet consists of the solid core of radius r and liquid film of thickness h, with the external radius of the droplet being R.

the thermodynamic theory contained in the present paper does not allow such coexistence of phases unless some rather unphysical dependence of interfacial tension on both composition and curvature are assumed. On the other hand, other features of the data are reproduced by the theory. Exactly what ingredients are missing must be left to further analysis, but as already mentioned, the uncertain state of the initial soluble particle could be a factor.

2. Thermodynamic Formulation

In accordance with the level of rigor outlined above, we present and discuss, in this section, the thermodynamic relations that will form the basis of our derivation. We consider a composite particle (Figure 2) consisting of a soluble crystalline core (phase γ) of radius r surrounded by a spherical film of liquid solution (phase α) of thickness h. The radius of the complex is denoted by $R = r + h$. Note that we are taking the liberty of representing the crystal as a spherical particle. The entire particle is surrounded by the vapor (phase β) of the solvent in the liquid film. The involatile solute in the film consists of molecules of the crystal core. The solvent is insoluble in the core.

The initial state of the system is chosen to be the "dry" crystal core in solvent vapor, and the "intermediate state" differs by having the core surrounded by the film of solution. (Note that the core will be smaller in the intermediate state because some of it will be dissolved in the film.) We need to express the change in the Gibbs free energy of the system in going from the initial to any intermediate state. This problem resembles that which is frequently encountered in the vapor phase nucleation theory[21] of a binary droplet, except for the fact that, in that case, the two components in the solution come from the vapor phase, whereas in the present case, the components in the liquid film come separately and respectively from the solid and vapor phases. In the binary droplet case, the change in free energy on forming the drop from the vapor is, within the confines of the capillarity approximation, given by

$$\Delta G = -\nu_1[\mu^{\beta}{}_1(P,\chi^{\beta}) - \mu^{\alpha}{}_1(P,\chi^{\alpha})] - \nu_2[\mu^{\beta}{}_2(P,\chi^{\beta}) - \mu^{\alpha}{}_2(P,\chi^{\alpha})] + \sigma^{\alpha\beta}S^{\alpha\beta} \quad (1)$$

where ν_1 and ν_2 are the numbers of molecules of components 1 and 2 in the drop and $\mu^{\alpha}{}_1$, $\mu^{\beta}{}_1$, $\mu^{\alpha}{}_2$, and $\mu^{\beta}{}_2$ are respectively the chemical potentials of component 1 in the drop, of component 1 in the vapor, of component 2 in the drop, and of component 2 in the vapor. P_1 and P_2 are the partial pressures of the components in the vapor mixture, whereas P is the total pressure of the vapor, and χ^{α} and $\chi^{\beta}$are the mole fractions of component 2 in the drop and the vapor, respectively. Finally, $\sigma^{\alpha\beta}$ is the surface tension of the drop, whereas $S^{\alpha\beta}$ is the area

of the interface between the drop and the vapor. The interface is regarded as sharp, the drop is regarded as incompressible, and surface excesses (adsorptions) are ignored; that is, it is assumed that neither of the components is surface active.

Adopting the same level of approximation in expressing ΔG for the formation of the intermediate state in the deliquescence problem, we can write

$$\Delta G = -\nu_1[\mu^{\beta}{}_1(P) - \mu^{\alpha}{}_1(P,\chi^{\alpha})] - \nu_2[\mu^{\gamma}{}_2(P) - \mu^{\alpha}{}_2(P,\chi^{\alpha})] + \sigma^{\alpha\beta}S^{\alpha\beta} + \sigma^{\alpha\gamma}S^{\alpha\gamma} - \sigma^{\gamma\beta}S^{\gamma\beta} \quad (2)$$

This expression differs from eq 1 in that *three* surface terms occur (corresponding respectively to the interface between the film α and the vapor β, the film α and the crystal γ, and the crystal γ and the vapor β) because two interfaces are formed when the intermediate state of the system is created, whereas another interface is destroyed along with the initial state, thus accounting for the minus sign before the last term in eq 2. The differences in square brackets depart from those in eq 1 in that both the β phase and the γ phase are represented, because now the components of the α phase come from those *two* other phases. In eq 2, component 2 is the solute originating in the crystal. In the solution, the solute molecules can dissociate into ions. In this case, χ^{α} will refer to the mean ionic mole fraction of component 2 in the solution (film). In the following, if the dissociation of solute molecules takes place, it will be assumed to be complete.

When this is the case, standard thermodynamic procedure[16] allows eq 2 to be written as

$$\Delta G = -\nu_1 \ln\left[\frac{\zeta}{(1-z\chi)f_1}\right] - \nu_2 z \ln\left[\frac{\chi^* f^*{}_2}{\chi f_2}\right] + \frac{1}{kT}(\sigma^{\alpha\beta}S^{\alpha\beta} + \sigma^{\alpha\gamma}S^{\alpha\gamma} - \sigma^{\gamma\beta}S^{\gamma\beta}) \quad (3)$$

(ΔG is from now on expressed in units kT), where $\chi = \nu_2/(\nu_1 + z\nu_2)$ and $x = \nu_2/(\nu_1 + \nu_2)$, whereas $z = z^- + z^+$ where z^- and z^+ are the numbers of negative and positive ions into which the solute dissociates. ζ is the saturation ratio of the vapor. Finally, the asterisk indicates quantities associated with a solution saturated with the solute, whereas f_1 and f_2 are the activity coefficients of solvent and solute in the solution (f_2 is the mean ionic activity coefficient of the ionizable solute).

Notice that in both eqs 1 and 2 the chemical potentials are evaluated at the pressure P in the vapor, even though in phases α and γ the actual pressures are P^{α} and P^{γ}. This results from the fact that the condensed phases are incompressible and the constraints on the system are such that it can only exchange work with the surroundings via the vapor phase. Both eqs 1 and 2 can be demonstrated exactly (for an incompressible system) using the full power of Gibbsian surface thermodynamics[16−19] or within the limits of the capillarity approximation using a "syringe method".[22] Of course, eq 1 should cause no debate because it has been used routinely in nucleation theory through the years. In both approaches, because intermediate states are generally not equilibrium states (not even states of unstable equilibrium), such states are treated as though they *were* equilibrium states, so that quantities such as surface tension can be given their customary meanings and so that the work of reaching an intermediate state can be considered reversible. This question is discussed at some length by Debenedetti and Reiss.[17,18] The point that we wish to emphasize is that a treatment of deliquescence based on eq 2 is essentially at the same level of approximation as the classical theory of nucleation (CNT) which has been capable of describing many qualitative features of measured nucleation phenomena and that our use of the treatment for the deliquescence case represents an attempt to demonstrate only the qualitative features of that phenomenon.

The actual pressure in the film α is obtained by using the Laplace relation[16] as

$$P^{\alpha} = P + 2\sigma^{\alpha\beta}/R \quad (4)$$

whereas that in the solid core is

$$P^{\gamma} = P + 2\sigma^{\alpha\beta}/R + 2\sigma^{\alpha\gamma}/r \quad (5)$$

Also the pressure in the "dry" crystal of radius r_0 surrounded by the vapor is

$$P^{\gamma}{}_0 = P + 2\sigma^{\gamma\beta}/r_0 \quad (6)$$

At this point, we note that if the film is very thin, i.e., $R \simeq r$, so that the nonuniform layers associated with the $\alpha\beta$ and $\alpha\gamma$ interfaces overlap, then "disjoining pressure"[15] must be taken into account. It can be shown (see the Appendix), assuming that there is no interfacial adsorption, that eq 3 must be replaced by

$$\Delta G = -\nu_1 \ln\left[\frac{\zeta}{(1-z\chi)f_1}\right] - \nu_2 z \ln\left[\frac{\chi^* f^*{}_2}{\chi f_2}\right] + \frac{1}{kT}(\sigma^{\alpha\beta}S^{\alpha\beta} + \sigma^{\alpha\gamma}S^{\alpha\gamma} - \sigma^{\gamma\beta}S^{\gamma\beta}) - \frac{\upsilon_1}{kT}\int_0^{\nu_1}\Pi(\chi, h)\,\mathrm{d}\nu_1|_{\chi=\text{const}} - \frac{\Delta\nu_2}{kT}\int_0^{\nu_2}\Pi(\chi, h)\,\mathrm{d}\nu_2|_{\chi=\text{const}} \quad (7)$$

where the υ's are the constant (incompressible) partial molecular volumes; υ_2 is understood as the sum of volumes of ions in which one solute molecule dissociates in the solution:

$$\upsilon_2 = z^-\upsilon_2{}^- + z^+\upsilon_2{}^+$$

with $\upsilon_2{}^-$ and $\upsilon_2{}^+$ being the corresponding partial ionic volumes; $\Delta\upsilon_2 = \upsilon_2 - \upsilon_2{}^{\gamma}$. The last two terms in eq 7 represent work associated with the disjoining pressure $\Pi(x, h)$, whereas h is the film thickness and these two last terms and the corresponding work represent the only differences between eqs 3 and 7, the result that is obvious on a physical basis alone.

3. Study of the Barrier: Nucleate or Activate Deliquescence and Vapor Phase Nucleation or Activation

Before proceeding further, it is convenient to set the stage by considering a somewhat more global scenario within which the position and influence of the deliquescence phenomenon can be easily understood. Consider an initial state of the system consisting of the dry soluble crystal and a surrounding solvent vapor, *undersaturated* with respect to pure solvent liquid. Then condensation to form an aerosol of pure solvent drops is not possible. However, deliquescence of the solid particles could still occur and result in a final state consisting of an aerosol of drops of liquid binary solution. Whether or not this occurs depends on several factors. First, there is the thermodynamic consideration that requires the final state to have a lower free energy than the initial one. Second, there is the matter of kinetics in which, even if deliquescence does involve a decrease of free energy, the process may involve a free energy barrier so that deliquescence may not occur in any reasonable time. Such free energy barriers are usually associated with interfaces and their accompanying free energies, of which three have been discussed

in the previous sections. If the dry solid particles are small enough, it is conceivable that the aerosol formed, immediately after the barrier is crossed, contains only partially dissolved solid cores, because further growth, into drops of solution without cores, would involve a second barrier originating in the work required to expand the outer surface of the drop. (However, we show below that this situation (partial dissolution) cannot occur if the solution behaves ideally.) Confining attention to the case where there is no secondary barrier, the passage of the system over the first barrier must proceed via the occurrence of fluctuations; it is essentially a "nucleation" process in which the product is a fully liquid drop resulting from deliquescence. It is convenient to refer to this process as "nucleate deliquescence". On the other hand, it is possible for the undersaturation to be mild enough so that the free energy barrier vanishes. Then we have the analogue of what, in vapor phase nucleation, has been called "Köhler activation",[1−3] and we might identify this process as "activate deliquescence".

If the solvent vapor is *supersaturated* so that vapor phase nucleation is possible, it is likely that activate deliquescence will always occur. In this case, however, there will still be a conventional nucleation barrier inhibiting the growth of the deliquesced particle (in which the core may or may not be fully dissolved) into a macroscopic drop, and fluctuations will control the rate at which the barrier is overcome. On the other hand, when the supersaturation is high enough, the barrier may disappear so that Köhler activation will occur in its conventional form. Which of these several processes occurs depends on the particular character of the free energy surface corresponding to a given system. Because our focus is not on nucleation, we will confine attention to that part of the free energy surface associated with deliquescence. This is specified by eq 7, where we have shown that ΔG can be regarded as a function of ν_1 and ν_2 or equivalently as a function of r and R, because the latter variables are functions of the former. Note that, as $\nu_1$and ν_2 increase during the process of dissolution of the core, R will increase, but r will decrease.

It is convenient to illustrate some of the above scenario by reference to a model system that might resemble (very roughly) an NaCl system. For this system, we choose

$$z = 2, \quad \nu_1 = 3 \times 10^{-23}\ \text{cm}^3, \qquad \nu_2 = \nu_2{}^{\gamma} = 2 \times 10^{-23}\ \text{cm}^3$$
$$f_1 = f_2 = 1, \quad x^* = 0.29, \qquad \zeta = 0.61, \quad T = 298.15\ \text{K}$$
$$\sigma^{\alpha\beta} = 72\ \text{dyne cm}^{-1}, \quad \sigma^{\alpha\gamma} = 276\ \text{dyne cm}^{-1}, \quad \sigma^{\beta\gamma} = \sigma^{\alpha\beta} + \sigma^{\alpha\gamma} \tag{8}$$

The last relation is just Young's equation[16] with zero contact angle. Note that we have taken the liberty of assuming the system to be ideal in the sense that the activity coefficients are set equal to unity. Note also that because $\zeta < 1$ the system of eq 8 cannot correspond to a case in which vapor phase nucleation of macroscopic drops of pure solvent can occur. For $\Pi(\chi, h)$, in eq 7, we adopt an expression similar to a semiempirical model proposed by Derjagin (see refs 15 and 23) and expressed by the following formula

$$\Pi(\chi, h) = (1 - x)K_1 e^{-h/l_1} + xK_2 e^{-h/l_2} \tag{9}$$

The values of the parameters that we used in this formula are

$$K_1 = 10^8\ \text{dyne/cm}^2, \quad l_1 = 2.3 \times 10^{-7}\ \text{cm}, \quad K_2 = 3 \times 10^9\ \text{dyne/cm}^2, \quad l_2 = 0.17 \times 10^{-7}\ \text{cm} \tag{10}$$

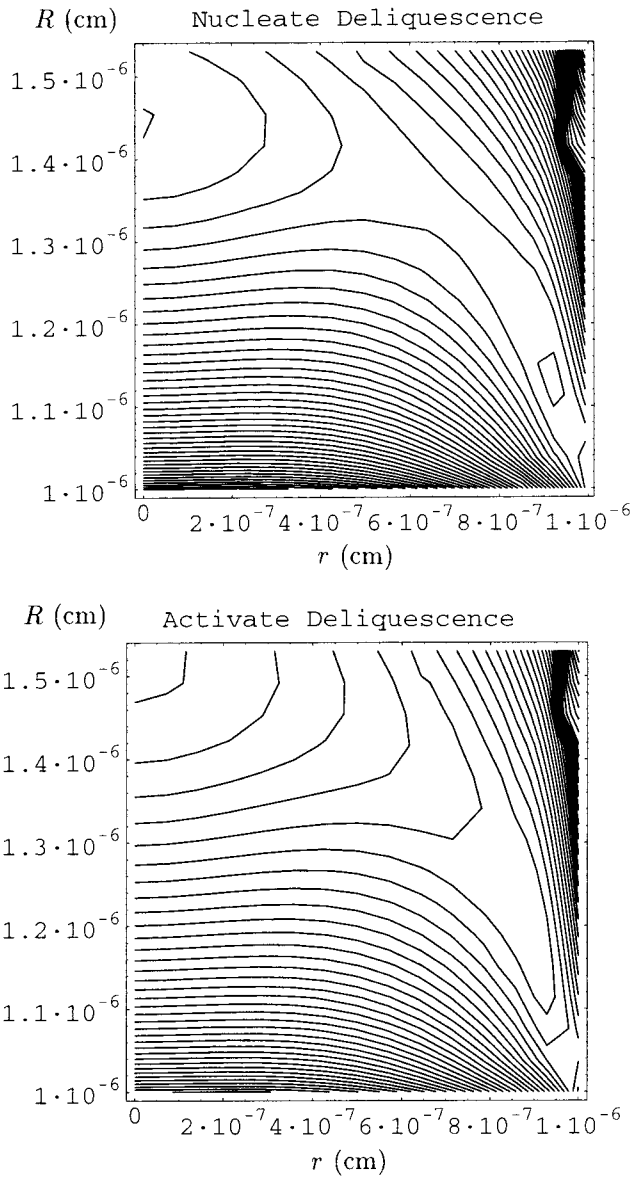

Figure 3. Contours of free energy surface for droplet formation on a model NaCl particle of initial radius $r_0 = 10$ nm in a water vapor at $T = 298.15$ K under conditions (17), when only deliquescence of particle occurs but formation of an irreversibly growing droplet is impossible. Case a corresponds to nucleate deliquescence at $\zeta = 0.61$, whereas case b represents activate deliquescence at $\zeta = 0.6618$. The initial state of the droplet corresponds to $r = R = r_0 = 10$ nm (dry particle).

For the system of eq 8, consider the free energy surface, corresponding to ΔG plotted as a function of r and R, which, in the absence of adsorption (see Appendix), can be chosen as the independent variables. We generate this surface using eq 7. The result, expressed in terms of r and R, is provided by the contour map in Figure 3a. This figure reveals some important features. If, for example, one moves upward along a vertical line fixed at $r = 6 \times 10^{-7}$ cm, the contour map shows that one first descends into a valley and then ascends on the opposing slope of the valley. If, instead, a vertical line fixed at $r = 9 \times 10^{-7}$ cm is traversed, a similar descent followed by an ascent is encountered; however, as the closed contour shows, the bottom of the valley along this line is also a "basin" on the free energy surface. If one moves to the left along the valley floor there is again an ascent. Because the basin forms a local minimum on the free energy surface, the system at its low point would be at least in metastable equilibrium; that is, there might

be a lower minimum at some other position. Actually, in the case represented by Figure 3a, there *is* another (lower) minimum that can be reached by moving (ascending) along the floor of the valley to and through the saddle point in the middle of the figure. Because the system must *ascend* to the saddle point, the path along the valley floor presents a free energy "barrier" so that the minimum on the other side can only be reached through the occurrence of a fluctuation; that is, the process is one of "nucleate deliquescence". In the case of Figure 3a, the minimum reached by this process is one in which $r = 0$, so that the solid core has fully deliquesced to a stable drop of solution.

A contour map for the case of "activate deliquescence" is shown in Figure 3b for which $\zeta = 0.662$. In this figure, starting from the lower right-hand corner and following the valley floor to the upper left-hand corner, the path is always downhill. Thus, the deliquescence is barrierless. Actually, $\zeta = 0.662$ is the value at which the barrier first disappears, and it therefore represents the critical saturation ratio for (Köhler-like) activation (for deliquescence) of the core particle.

If $\zeta > 1$ so that the vapor is supersaturated with respect to pure solvent liquid, deliquesced particles can grow irreversibly into macroscopic drops of pure solvent; that is, vapor phase "nucleation" of a solvent aerosol is possible. We do not present a contour plot for this case (which, as indicated above, could involve a secondary barrier) but, instead, proceed to a generic but more quantitative analysis of the two cases, $\zeta < 1$ and $\zeta > 1$, focusing only on deliquescence.

Before proceeding to this discussion, we note that, if the time for the fluctuation of material between core and film is much longer than that for fluctuation between vapor and film, the core may be momentarily treated as an insoluble particle surrounded by a layer of solution, and the rate controlling process will then be the dissolution of the core. That the relative time scales are in this ratio is plausible because dissolution requires the breaking of crystal "bonds", whereas condensation does not involve this process.

Returning to the analysis, we first address the dependence of ΔG on R when r is held fixed. Because we have assumed the absence of surface active species in the film and have neglected interfacial adsorptions (see the Appendix), the first partial derivative of ΔG with respect to R, at constant r, may be written as

$$\frac{\partial \Delta G}{\partial R} = \frac{\partial \Delta G}{\partial \nu_1}\frac{\partial \nu_1}{\partial R} \tag{11}$$

Using eqs A1, A7, A13, and A15 (see the Appendix), we obtain

$$\frac{\partial \Delta G}{\partial R} = \frac{4\pi R^2}{\upsilon_1}(\phi^\alpha - \ln \zeta) \tag{12}$$

$$\phi^\alpha \equiv \phi^\alpha(r, R) = \frac{\upsilon_1}{kT}\left[\frac{\sigma^{\alpha\beta}}{R} - \Pi(r, R)\right] - \ln\left[\left(1 + z\frac{\upsilon_1}{\upsilon_2}\frac{r_0{}^3 - r^3}{R^3 - r_0{}^3 - (r_0{}^3 - r^3)\Delta\upsilon_2/\upsilon_2{}^\gamma}\right)/\ln f_1(r, R)\right] \tag{13}$$

in which $\Pi(r, R) \equiv \Pi(\chi(r, R), h(r, R))$ and $f_1(r, R) \equiv f_1(\chi(r, R))$ are the disjoining pressure and activity coefficient of component 1 expressed in terms of r and R. As is easy to show (see the Appendix), ϕ^α is the displacement of the chemical potential of component 1 in the film from its equilibrium value, $\mu_{1\infty} \equiv \mu_{1\infty}{}^\alpha = \mu_{1\infty}{}^\beta$, expressed in units k_BT. Figure 4 shows a typical dependence of ϕ^α on R at fixed r. In constructing this

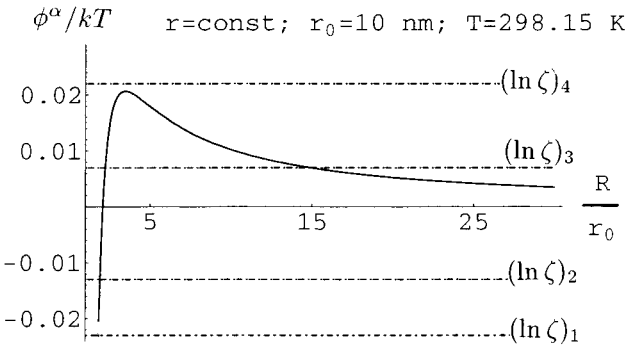

Figure 4. Typical behavior of the function ϕ^α versus the external radius R of the droplet, at some fixed internal radius r of the film ($r = 0.9r_0$). The example of a model NaCl particle of initial radius $r_0 = 10$ nm in a water vapor at $T = 298.15$ K is considered.

figure, we made use of the values of some of the parameters listed in eqs 8 and 10. Because, for a not too small particle, the disjoining pressure dominates the capillary pressure (both having large but finite magnitudes) as $R \rightarrow r_0$, and at the same time the last term on the right of eq 13 tends to some negative value, it can be concluded that ϕ^α tends to some relatively large negative value $\phi^\alpha{}_{\min}$ as $R \rightarrow r_0$. This is evident in Figure 4 which also shows that ϕ^α has a positive maximum $\phi^\alpha{}_{\max}$ at some $R^* \equiv R^*(r)$ and tends to zero as $R \rightarrow \infty$ (we assume that the minimum thickness of the film is that of a monolayer). We examine four cases at fixed r. The first two of these cases correspond to the situation in which $\zeta < 1$, so that only deliquescence (nucleate or activate) can occur and vapor phase nucleation or activation is ruled out.

Case 1. $\zeta < 1$ and the vapor is sufficiently undersaturated so that

$$\ln \zeta \le \phi^\alpha{}_{\min} \tag{14}$$

Then, because $\ln \zeta$ is independent of r and R, it may be concluded from eq 12 that $\partial\Delta G/R > 0$ for all $R > r_0$; that is, the free energy ΔG will increase monotonically with increasing R at any fixed r. This case can be represented by the horizontal dashed line labeled $(\ln \zeta)_1$ in Figure 4. This line nowhere intersects the curve ϕ^α. Thus, with regard to Figure 3a, this is a case in which there is no valley so that the free energy surface slopes upward, everywhere. In this case, *no deliquescence*, either nucleate or activate, is possible and the solid core remains dry.

Case 2. $\zeta < 1$, but the vapor is not as undersaturated as in Case 1, so that

$$\phi^\alpha{}_{\min} < \ln \zeta \le 0 \tag{15}$$

This case is represented in Figure 4 by the horizontal line labeled $(\ln \zeta)_2$ which intersects the ϕ^α curve at only one value of R that we denote as $R_e \equiv R_e(r)$ so that eq 12 requires

$$\left.\frac{\partial \Delta G}{\partial R}\right|_{R_e} = 0 \tag{16}$$

The extremum of ΔG at $R \equiv R_e(r)$ must correspond to a minimum because, according to eqs 12 and 13, together with the fact that $\ln \zeta$ does not depend on R, $\partial\Delta G/R$ must be negative for $R < R_e$ and positive for $R > R_e$. This is the case in which the free energy surface possesses a "valley", as in Figure 3a, and the minimum occurs (at the valley floor) as the valley is crossed. If ζ is such that a barrier exists on the path along the valley floor, then deliquescence can occur, but it will be of the "nucleate" variety. If ζ is sufficiently large, although still less

than unity, the floor of the valley will slope downward with decreasing r, so that deliquescence will be barrierless, i.e., it will be "activate", and the situation will correspond to Figure 3b. Finally, if the minimum occurs in the "basin" exhibited in Figure 3a, then nucleate deliquescence can still occur, but a metastable "partial deliquescence" could occur such that the core will only be partially dissolved. Note that soluble particles such as NaCl, when they are large enough, always deliquesce fully with a value of $\zeta < 1$ or $\ln \zeta < 0$, satisfying the upper bound in eq 15, and therefore form an example of case 2. An assembly of such particles constitutes a stable binary aerosol. It is worth mentioning, in connection with the basin, that it does not occur if the disjoining pressure is neglected and, in the following section, more will be said on this issue when theory is compared with the experiments of Hämeri et al.[14]

The next two cases correspond to the situation in which the vapor is supersaturated, i.e., to $\zeta > 1$. Under this condition, vapor phase nucleation or activation can occur. We do not show contour maps for this situation.

Case 3. The vapor is supersaturated so that

$$0 < \ln\zeta < \phi^{\alpha}{}_{\max} \tag{17}$$

This case is represented by the horizontal line labeled $(\ln \zeta)_3$ in Figure 4. The line intersects the curve ϕ^{α} in two places. The intersection at the smaller value of R clearly corresponds to a minimum of ΔG (for the same reason as in case 2; that is, the intersection occurs where ϕ^{α} has a positive slope), whereas that at the larger value of R corresponds to a maximum (because the intersection occurs where ϕ^{α} has a negative slope). A vertical line on a contour map corresponding to this case would first cross a valley (the minimum) and then ascend the opposing slope of the valley to reach a maximum. The descent, beyond this maximum, could lead to the formation of a macroscopic drop of solvent, if the supersaturation was sufficiently large to support Köhler activation, or at least vapor phase nucleation if ζ was not large enough to cause activation. If the saddle point along the floor of the valley was higher than the maximum along the vertical line, then the path to nucleation along the vertical line would be preferred over that through the saddle.

Case 4. The vapor is sufficiently supersaturated so that

$$\ln \zeta > \phi^{\alpha}{}_{\max} \tag{18}$$

This case is represented in the figure by the horizontal line labeled $(\ln \zeta)_4$, a line that again does not intersect the curve ϕ^{α}. Because there is no intersection, and eq 18 holds, eq 12 requires $\partial \Delta G/R < 0$ for any given r, and hence, the free energy of the droplet decreases monotonically with increasing R, beginning at $R = r_0$. In this case, we would have Köhler activation because the nucleation barrier would no longer exist at the high level of supersaturation under consideration.

In the following section, the theory and its consequences, as exhibited in both the contour maps of Figure 3a,b and the four cases studied above, are compared to the experiments that have been performed using both electrodynamic levitation[11,12] and the tandem differential mobility analyzer.[14,20]

4. Comparison of Theory and Experiments

4.1. Experiments. The experiments were performed using a tandem differential mobility analyzer (TDMA). A detailed description of the experimental setup was presented by Hämeri et al.,[14] and only a short summary is presented in the following. The TDMA is a flow setup based on use of two differential mobility analyzers (DMA). The first DMA is used as a classifier, which separates a monodisperse fraction of the aerosol. The flows in the first DMA were dried to less than 5% relative humidity (typically 2%). After classification, the monodisperse aerosol was humidified to a controlled RH and the particle size was determined using the second DMA. The humidity in this DMA was controlled and determined by means of a chilled mirror dew point hygrometer, and the DMA temperature was stabilized at 24 °C. Particles were counted using a condensation particle counter (3010, TSI Inc.).

Aerosol particles were generated by atomization of solution droplets into the air stream. Dilute solutions of distilled water and ammonium sulfate or sodium chloride were prepared by mixing 0.1 g of salt with 1 L of water. The solution droplets were dried by mixing with air-dried with a silica gel drier.

The monodisperse data could be characterized as a narrow triangular shaped size distribution. As the particles grow the shape of the distribution remains similar and only a slight broadening can be observed due to slightly different growth characteristics of the particles representing the upper and lower ends of the size distribution. Measurements were started at low relative humidities, and the RH was gradually increased to allow for determination of water adsorption onto the particle surfaces. At the RH of deliquescence, particles grew rapidly to sizes much larger than the original dry radius. However, near the RH range of deliquescence, some particles sometimes grew significantly, whereas others remained close to the dry size. This is indicative of slightly different relative humidity histories for these two particle groups inside the TDMA system. The two groups were consequently analyzed separately, and two data points were obtained. During deliquescence, some data points were found to be clearly between the dry and fully deliquesced radius. Such data points corresponded to well defined and rather narrow size distributions and did not represent any "average" behavior of a mixed group of dry and fully deliquesced particles.

Inaccuracy in the experimental data results both from determinations of the particle size and of relative humidity. The question of accuracy of the experimental data has been examined in previous papers.[14,20] It was found that the greatest inaccuracy was associated with the determination of the relative humidity inside the second DMA and was maximally $\pm$ 1%. The determination of particle size is most sensitive to changes of the flow rates inside the DMAs. Flows were controlled using mass flow controllers and were calibrated, after each change in the RH set point, prior to a succeeding measurement.

Because the DMA method is based on the determination of particle mobility, the particle radius obtained is a "mobility equivalent" radius. The dry particles are not spherical and the particle shape should really be considered when analyzing the data. In addition, the drying process during the particle generation could produce particles with densities that differ from the bulk density value. These effects were also considered by Hämeri et al.[14,20] Measurements using relatively large particles (15−25 nm in radius) show good agreement with both theory and other measurements, and therefore, the major scatter in the small particle data is considered to be due to the aerosol particle properties and the growth process rather than to experimental inaccuracy. Specifically, it appears that smaller dry particles, have lower densities, because of voids in the crystal structure that result perhaps from multiple nucleation events and/or imperfect crystal growth when the atomized droplets are dried. These effects are especially pronounced with NaCl.

4.2. Free Energy Profile along the "Valley Floor". The experiments on the deliquescence of small particles[14,20] were

performed under the conditions of case 2 in the preceding section and, therefore, on free energy surfaces resembling those of Figure 3a,b. These conditions allow either nucleate or activate deliquescence but, because $\zeta < 1$, do not allow either vapor phase nucleation or activation. The results[14] of such an experiment with $(NH_4)_2SO_4$ as the soluble core are shown in Figure 1, where the increase of particle mass (because of the uptake of water) is plotted as a function of relative humidity ($\zeta \times 100$) for two initial core sizes. The foregoing theory will now be used in an attempt to explain the *qualitative* features of these plots.

We begin with the assumption that the deliquescence process, nucleate or activate, proceeds along the path of lowest ΔG on the floors of the valleys shown in Figure 3a,b. A particle on this path may be considered to be in quasiequilibrium with the vapor phase, leaning on the idea mentioned earlier that the exchange of material between the solid core and the liquid film is expected to be much slower than that between vapor and film. Again, this idea stems from the fact that the exchange with the solid core involves the breaking or creating of crystal bonds, so that the energy of activation for the relevant kinetic processes should be larger than that for the condensation of water molecules onto the film. This situation is reminiscent of the process of binary nucleation in vapor mixtures of water and sulfuric acid.[24] In that case, on the time scale of the exchange of water between the vapor and the developing sulfuric acid−water embryo, the acid behaves as an involatile solute.[25]

Clearly then, if the solute content of the film is fixed on the time scale of its exchange of molecules with the vapor, r must be constant and quasiequilibrium with water must occur at the minimum value of ΔG along a vertical line on a contour map such as those in Figure 3a,b. However, this minimum is a point on the lowest free energy path on the floor of the valley, and the continuum of such points must be the path of lowest free energy.

We can calculate ΔG which we denote as $\Delta G'$ along this path. To do this, we first make use of eqs 12, 13, and 16. Substituting eqs 12 and 13 into eq 16, we obtain

$$\ln \zeta + \ln\left[1 + z\frac{v_1}{v_2}\frac{{r_0}^3 - r^3}{R^3 - {r_0}^3 - ({r_0}^3 - r^3)\Delta v_2/{v_2}^{\gamma}}\right] - \ln f_1(r, R) = \frac{v_1}{kT}\left[\frac{\sigma^{\alpha\beta}}{R} - \Pi(r, R)\right] \quad (19)$$

The solution of this equation, $R = R_e(r)$, describes the minimum free energy path. To obtain an expression for $\Delta G'$ itself along this path, we integrate along the path, using eq A12. In performing this integration, we note that v_2 and r are related by eq A2. Also, making use of eqs A14 and A16, we find

$$\Delta G' = \frac{4\pi({r^3} - {r_0}^3)}{3{v^{\gamma}}_2} z \ln(\chi^* f^*_2) + \frac{1}{kT}\sigma^{\alpha\gamma} 4\pi({r^2} - {r_0}^2) - \frac{4\pi z}{{v^{\gamma}}_2}\int_r^{r_0}\left[\ln\left(z + \frac{{v^{\gamma}}_2}{v_1}\frac{{R^3}_e(r') - {r_0}^3 - ({r_0}^3 - r'^3)\Delta v_2/{v_2}^{\gamma}}{{r_0}^3 - r'^3}\right) - \ln f_2(r, R_e(r'))\right] r'^2\, dr' + \frac{4\pi}{kT}\frac{\Delta v_2}{{v_2}^{\gamma}} \times \int_r^{r_0}\left[\frac{2\sigma^{\alpha\beta}}{R_e(r')} - \Pi(r', R_e(r'))\right] r'^2\, dr' \quad (20)$$

in which we have expressed $\Delta G'$ as a function of r rather than R, but the two radii are related by $R = R_e(r)$ (see eq 19).

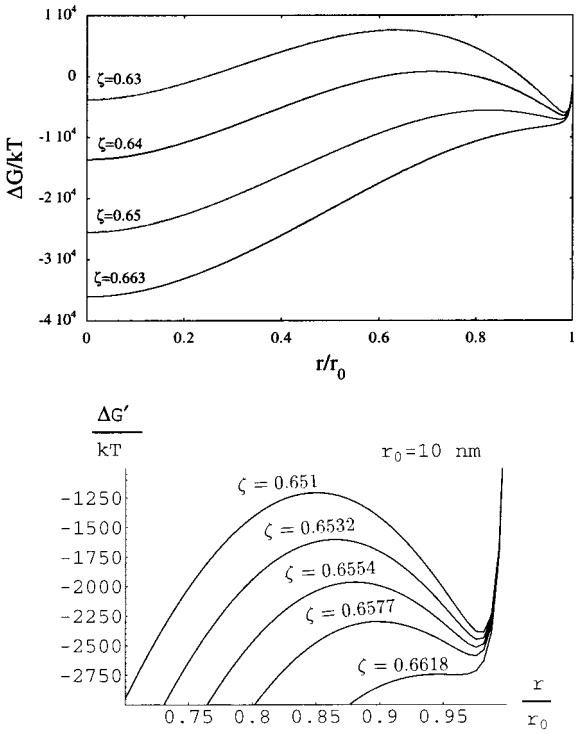

Figure 5. Free energy barrier profile on the path along the valley floor of the free energy surface, i.e., $\Delta G'$ versus r (eq 20). (a) A general behavior; (b) the example of the model NaCl particle of initial radius $r_0 = 10$ nm in a water vapor at $T = 298.15$ K is considered. The curves are given at different saturation ratios of the water vapor indicated above the respective curve. The lowest curve corresponds to the activation of deliquescence occurring at $\zeta = 0.6618$, whereas the four upper curves represent the nucleate deliquescence of the particle.

4.3. Numerical Results Based on Theory for an Ideal Film. As a simple example of our procedure, we first attempt to calculate $\Delta G'$, assuming the film solution to be ideal, so that we can use the parameters and relations of eq 8. Results appear in Figure 5a which shows $\Delta G'$ as a function of r, for different values of the saturation ratio ζ. r_0 was chosen nominally to be 10 nm. The initial dry particle undergoes immediate deliquescence and falls to a minimum on the free energy surface. This minimum corresponds simply to the passage of the path through the "basin", discussed in section 4 in connection with Figure 3a. However, as already discussed in section 4, the minimum implies that the particle deliquesces only partially and arrives at an equilibrium involving an only slightly dissolved core surrounded by a thin film of solution. At this point, $\partial\Delta G/R = \Delta G/r = 0$.

If the partially deliquesced state is more stable than the fully deliquesced one, then the equilibrium is stable; otherwise, it is metastable. The curve for $\zeta = 0.63$ in Figure 5a shows that the minimum at this value of ζ is "stable" because $\Delta G'$ in the fully deliquesced state ($r = 0$) is higher than at the minimum near $r/r_0 = 1$. However, on the curves for $\zeta = 0.64$ and 0.65, $\Delta G'$ at the minimum lies higher than at $r = 0$, so that on these curves, the equilibrium corresponding to the partially deliquesced state is "metastable". On the curve for $\zeta = 0.663$, the minimum has disappeared. Thus, there is no barrier between the partially deliquesced and fully deliquesced states, and the deliquescence, in this case, is clearly "activate" rather than "nucleate". However, in the case of the preceding three curves, a barrier exists and so the deliquescence is of the "nucleate" variety.

It should be reemphasized that the basin and the associated minimum, as well as the phenomenon of partial deliquescence,

represent effects due to the disjoining pressure that acts to reduce $\Delta G'$. Without the disjoining pressure, we would not expect to observe partial deliquescence. To determine the critical value of ζ for the occurrence of activate nucleation, a more highly resolved study of the effect of ζ on plots of $\Delta G'$ versus r was performed for the system involved in Figure 5a. The results of this study are shown in Figure 5b where curves similar to those in Figure 5a are shown but where ζ only varies between 0.6510 and 0.6618. The critical value seems to lie near $0.6618 \simeq 0.662$, the saturation ratio quoted in connection with Figure 3b. In the comparison of theory with experiment,[14] we have elected to focus on activate rather than nucleate deliquescence so as to avoid having to construct a difficult kinetic theory of rate. It is hoped that this simpler approach will still reveal the qualitative features of the experimental results.

In this respect, consideration of Figure 5a shows that our theory captures the mechanism for the observed[11−14,20] hysteresis of deliquescence−efflorescence curves. At the deliquescence point, now defined as ζ_{th}, the threshold value of ζ at which the barrier to deliquescence disappears, the fully deliquesced drop is considerably more stable than the dry particle (see Figure 5a). When an attempt is made to reverse the process, and ζ is decreased below ζ_{th}, the deliquesced drop persists in being the most stable, so that efflorescence does not occur. Even when the drop is not the most stable, i.e., when it is only metastable relative to the dry particle (see the curve for $\zeta = 0.63$ in Figure 5a), efflorescence may still not occur because of the "reverse" free energy barrier. Indeed, the drop does not effloresce until ζ is so low, and the solution within the drop is so concentrated, that nucleation of the crystal at a finite rate becomes possible.[11−14,20]

As already indicated, the results of some of the experiments, due to Hämeri et al.[14] involving water vapor and very small $(NH_4)_2SO_4$ core particles, and with which we want to compare our theory, are reproduced in Figure 1. Plotted in the figure is the ratio (growth factor) of the (apparent) equilibrium radius of the deliquesced particle to the radius of the initial core particle, i.e., R/r_0 (where R is assumed to be an outer equilibrium radius of the particle, composite or not), versus RH given by $\zeta \times 100$. Results for two different initial core radii, 5 and 7.5 nm, are shown, and several features of these data should be noted:

1. Initial uptake of solvent. As RH is increased, at first, the particle accumulates water gradually, but eventually, a value of RH is reached at which the growth factor increases rather abruptly, although at this point the curves do not exhibit a sharp discontinuity in slope in order to rise vertically.

2. Point of abrupt growth. The value of RH at which the sharp increase in growth factor occurs is larger for the larger core particle; for the 7.5 nm particle, this RH is about 80, whereas for the 5 nm particle, it is about 75.

3. Steepness of abrupt growth. The steepness of the sharp increase in growth factor increases with initial growth size. For example, in the case of the 7.5 nm core, the rise is almost vertical, whereas it is more gentle for the 5 nm core. In this connection, Hämeri et al.[14] studied cores with initial radii as large as 25 nm. The results for this case are shown in Figure 6, and the most notable feature is that the sharp rise is almost vertical. This implies that when the initial core lies in the micron size range, the rise should be indistinguishable from the vertical, and this is indeed what Tang and Munkelwitz[12] observed, giving the impression that the deliquescence was prompt in the sense of the theory of MRB.

4. Nominal RH range in which deliquescence occurs. In Figures 1 and 6, and in the studies (not shown here) of 4 nm ammonium sulfate particles by Hämeri et al.,[14] the deliquescence phenomena are localized to the saturation range 75−85 RH.

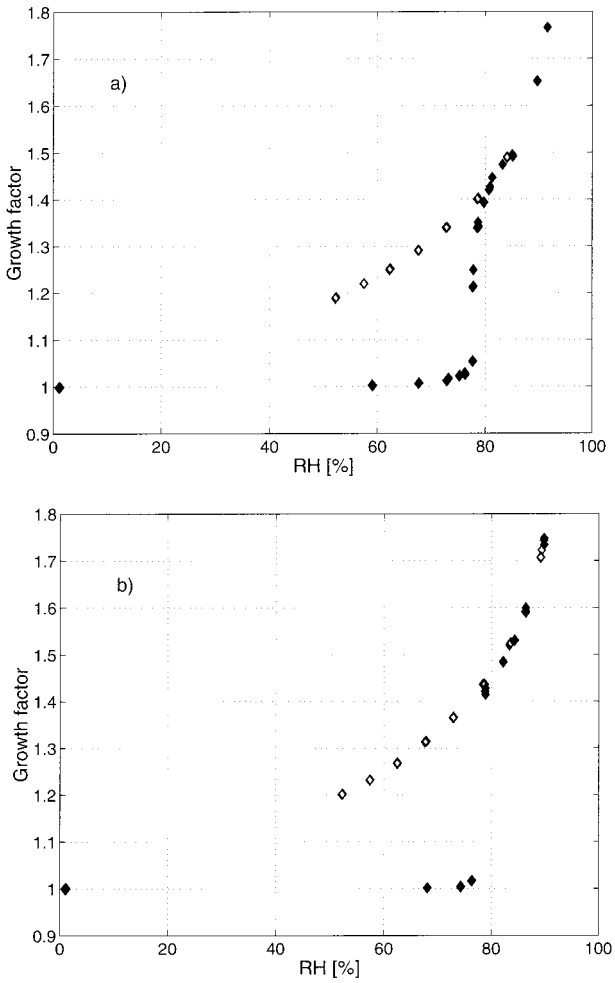

Figure 6. Growth factor, R/r_0, as a function of relative humidity, RH $= \zeta \times 100\%$, for $(NH_4)_2SO_4$ particles of dry radii: (a) $r_0 = 15$ nm and (b) $r_0 = 25$ nm. The data at increasing RH are indicated by the solid black symbols, and the data at decreasing RH are shown by open symbols.

It is convenient to focus our comparison of theory and experiment on the above features of the data. Before doing this, it is necessary to use the theory to calculate the relevant experimental curves. For this purpose, we use the parameters of eq 8. We cannot expect meaningful semiquantitative agreement between experiment and theory, although we can hope that the theory will reproduce many of the qualitative features of the experiment. In attempting to generate curves such as those in Figures 1 and 6, we assume the deliquescence path to lie along the valley minimum. Using this set of rules, we first consider item 1, above, "initial uptake of solvent".

We consider the equilibrium, associated with this initial uptake, to correspond to the entrapment of the system in the "basin" on the contour map of Figure 5a,b. In this minimum, the particle consists of a partly dissolved core surrounded by a layer of solution. The water in this solution represents the "uptake". As ζ or RH is increased, the minimum gradually moves to smaller values of r and larger values of R (see Figure 5a,b) from which we can determine a growth factor R/r_0, that gradually increases with increasing RH, and which can be plotted versus RH as in the case of the experiments (see Figures 1 and 6). It should be emphasized that the behavior of the basin and therefore of the initial uptake is largely due to the disjoining pressure.

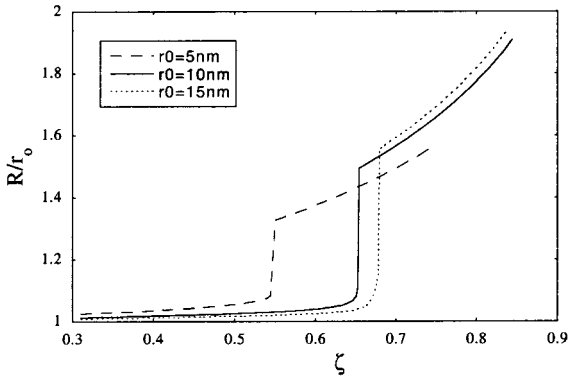

Figure 7. Theoretical predictions for the particle growth factor (the radius of particle at given RH divided by radius of particle at RH < 5%) versus saturation ratio, for model NaCl particles (in the case of ideal solution in the film).

As the RH is increased further, a point is reached at which the free energy barrier, inhibiting complete deliquescence, vanishes, so that the threshold value of ζ or RH is attained. We define this value of RH as the "deliquescence point" because we consider only activate deliquescence and neglect the nucleate variety. At this point, therefore, the core is assumed to dissolve "promptly", so that the plot of growth factor versus RH takes a vertical jump. After the core is fully deliquesced, the plot of growth factor versus RH is governed by the Kelvin equation for a binary drop containing an involatile solute.

In this way, the curves, corresponding to initial core radii of 5, 10, and 15 nm, appearing in Figure 7, were calculated.

We may now compare them with the four features of the experimental curves, discussed above. The first feature "initial uptake" has already been discussed, and we can see, in each of the curves of Figure 7, that there is a gradual initial uptake and a larger RH for abrupt growth is required for a larger initial core.

The second feature "point of abrupt growth" also occurs in the theory curves of Figure 7.

The third feature "steepness of sharp growth" is not described by the theory curves, because the sharp increase in slope is both discontinuous and vertical. In contrast, the experimental curves show a softer behavior without a discontinuity of slope and with a less than a vertical rise after the point of sharp growth is reached. However, Figure 7 suggests by extrapolation that as the initial core size is increased discontinuity and verticality will occur, a presumption that is borne out by the experiments of Tang and Munkelwitz[12] on micron size cores.

The fourth feature "nominal RH range in which deliquescence occurs" is reproduced roughly by the curves of Figure 7. We see that the range is about 60−70 RH as compared to the 75−85 RH in Figures 1 and 7. This agreement is certainly acceptable, given the crudeness of the theory and the fact that cores consisting of different salts are involved.

In the end, we see that the theory has not fully reproduced the experimental results. This is hardly surprising in view of the approximations that we have had to make in order to have a first theory of manageable simplicity. On the other hand, a number of the qualitative features of the phenomenon *are* reproduced, so that we can hope that increasingly refined theories will describe experimental behavior with increasing accuracy.

The demonstration, by the theory, of some of the qualitative features of the experiment prompts the question as to what must be added to the theory to demonstrate all of the features of the experiment. In this connection, it should be pointed out that Hämeri et al.[14] offered a discursive interpretation of their results that was not far from the more analytical discussion contained in the theory of this paper. These authors suggested that, for small sizes, the departure of their data from the simple Kelvin relation was due to a more generalized "Kelvin effect" that included the size dependence of the solubility of the crystal and, in addition, the dependence of surface tension on concentration and the nonideality of the solution. This is just another way of referring to the effects of surface on the thermodynamics of small particles, the subject addressed by MRB and the current paper.

In the case of ammonium sulfate experiment, Hämeri et al.[14] actually measured points that appear to correspond to equilibrium states along the sharply rising parts of the curves in Figures 1 and 6. In contrast, the curves shown in Figure 7, calculated from the theory of this paper, exhibit a rise that corresponds to a vertical jump between equilibrium states and no intermediate states along the path of the rise.

Perhaps, the most serious flaws in the foregoing analysis are the assumptions that the film can be treated as an ideal solution and that surface excesses can be ignored. If the activity coefficients and surface excesses were to be indeed included, then perhaps curves such as those in the experimental data without "vertical jumps" would be obtained. We elaborate one of these issues, nonideality, in subsection 4.4.

In closing this subsection, it should be noted that Hämeri et al.[14] argued that the slow initial increase in growth factor was due to the adsorption of water by the dry crystal. The present theory explains this portion of the curve as a limited dissolution of the crystal induced by the disjoining pressure, but the two effects are not so dissimilar.

4.4. Numerical Results and Comparison with Experiments for NaCl−H_2O Based on Theory for a Nonideal Film. Hämeri et al.[20] performed TDMA experiments on NaCl particles. Some of their data are reproduced by Figures 8−12. Enough is known about the thermodynamic parameters of the NaCl−H_2O system, especially solution activity coefficients, densities, etc. to prompt an attempt to generate a semiquantitative theoretical description of the deliquescence features of this system, taking into account nonideal behavior. Such an analysis is performed in the present subsection.

Rather than considering the full surfaces corresponding to ΔG the free energy of formation of intermediate states of deliquescence, it is now sufficient to focus on the thermodynamic relations that apply to states of equilibrium coexistence between crystalline core, film, and vapor, because the experimental data seem to apply to the system in a continuum of such states. Thus, we try to find numerical solutions in which the chemical potentials of NaCl and H_2O, in the film, are respectively equal to the chemical potentials of NaCl in the core and H_2O in the vapor.

The numerical calculations were carried out by iteratively solving the equations describing this equilibrium between water vapor, the liquid film, and the partially dissolved NaCl crystal. As follows from eqs A13 and A15, the equilibrium between water vapor and the liquid film on the partially dissolved crystal is characterized by

$$\zeta = a_1 \exp\left[\frac{v_1}{kT}\left(\frac{2\sigma^{\alpha\beta}}{R} - \Pi(r, R)\right)\right] \qquad (21)$$

Here, a_1 denotes water activity in the liquid film, and it was obtained from the experimental correlation of Tang et al.[11] The surface tension was determined using the correlation presented by Pruppacher and Klett,[26] and the density of the liquid film,

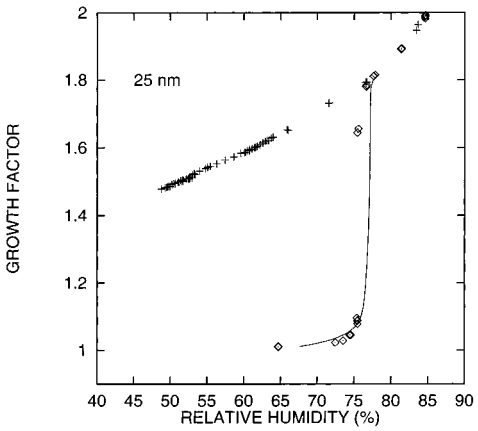

Figure 8. Particle growth factor (the radius of particle at given RH divided by the radius of particle at RH < 5%) versus relative humidity (the case of nonideal solution in the film). Dry particle radius $r_0 = 25$ nm. Diamonds: measurements at increasing RH. Crosses: measurements at decreasing RH. Solid line: theory.

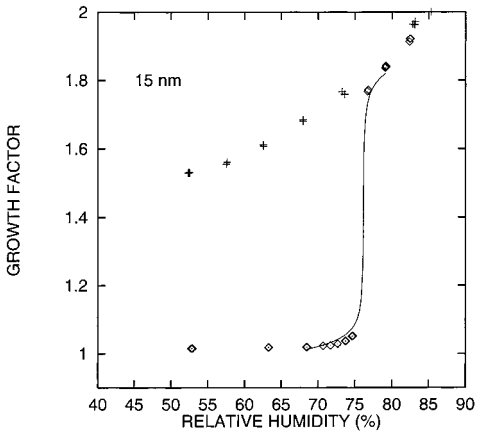

Figure 9. Same as that for Figure 8, except for $r_0 = 15$ nm.

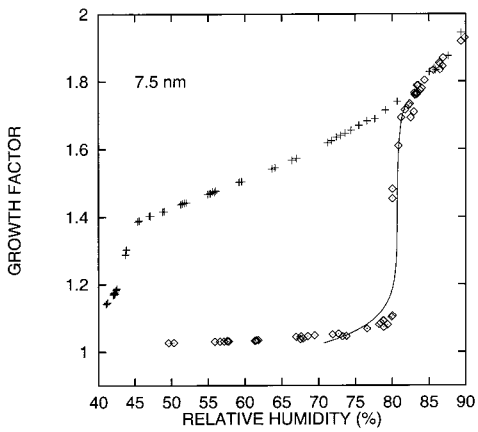

Figure 10. Same as that for Figure 8, except for $r_0 = 7.5$ nm.

used in calculation of the partial molecular volume, was obtained from a fitting to the data of CRC[27] presented by Hämeri et al.[20]

It follows from eqs A14 and A16 that the equilibrium of NaCl between the partially dissolved core and the film is characterized by

$$a_2 = a_2^* \exp\left[\frac{2\sigma^{\alpha\gamma}\upsilon_2^{\gamma}}{kTr} + \frac{\Delta\upsilon_2}{kT}\left(\frac{2\sigma^{\alpha\beta}}{R} - \Pi(r, R)\right)\right] \quad (22)$$

The NaCl activities in the film and in the saturated bulk solution, a_2 and a_2^*, were calculated using the model of Bromley.[28]

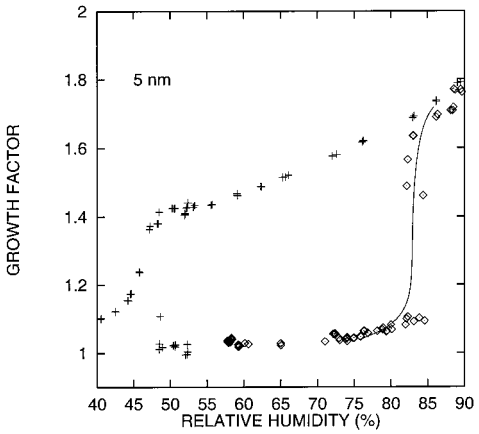

Figure 11. Same as that for Figure 8, except for $r_0 = 5$ nm.

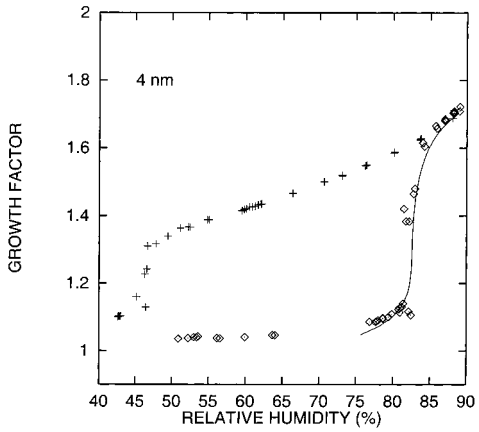

Figure 12. Same as that for Figure 8, except for $r_0 = 4$ nm.

The balance of salt molecules between crystal and film is accounted for by eq A1 which is rewritten here in the form

$$r_0^3 = r^3 + (R^3 - r^3)\frac{\upsilon_2^{\gamma}\chi}{\upsilon_1(1 - z\chi) + \upsilon_2\chi} \quad (23)$$

Note that the undissolved crystals are cubic rather than spherical in shape and that the smallest particles appear to contain significant void fractions (see subsection 4.1). This was taken into account by using the experimentally determined dry particle densities presented by Hämeri et al.[20] where appropriate (i.e. when the total number of NaCl molecules in the system was considered; however, the molecular volume υ_2^{γ} in eqs 22 and 23 was obtained from the bulk NaCl density).

It was very quickly found that, to reproduce the measurements, the crystal interfacial tension has to be regarded as a quantity dependent on crystal size and therefore also (implicitly) on solution composition. We found by the method of trial and error that the following formula can be applied in reproducing the empirical deliquescence data:

$$\sigma^{\beta\gamma} = y\left(\frac{r}{r + \Delta}\right)^3 \quad (24)$$

where y and Δ are adjustable parameters, which had to be determined separately for each dry crystal size. It is hard to justify this form physically, except in some rather unphysical limits. For example, if $\Delta \ll r$, then an expansion of eq 24 would yield $\sigma^{\beta\gamma} = y(1 - 3\Delta/r)$. If y is the surface tension for a plane interface, then Δ would be $2\delta/3$ where δ is the Tolman length.[29] Composition would also play a role.

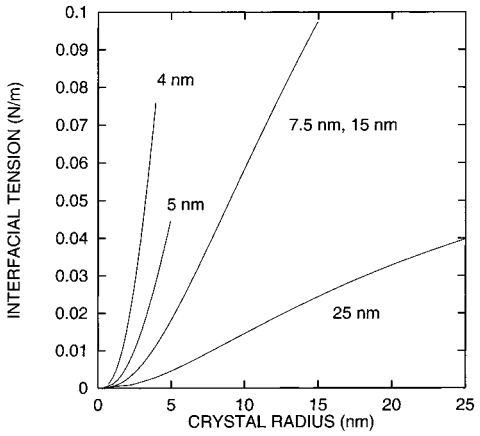

Figure 13. $\sigma^{\beta\gamma}$ (N/m) as a function of crystal radius (Å). The dry crystal sizes are indicated in the figure.

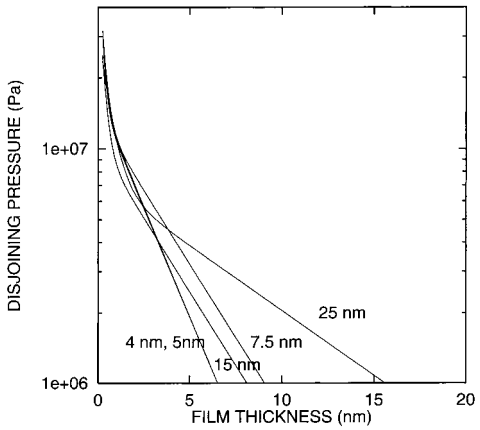

Figure 14. $\Pi(r, R)$ (Pa) as a function of the film thickness (Å). The dry crystal sizes are indicated in the figure. The vertical and horizontal scales were limited for clarity.

Figures 8−12 show the comparison between experiment results and theory calculations. It is seen that the theoretical curves fit the datapoints extremely well. However, as we indicated earlier, the fact that we had to resort to somewhat unphysical nonunique function for the crystal interfacial tension clearly indicates that some qualitative feature is still missing from the theory. Furthermore, the parameters of the disjoining pressure function (eq 9) had to be adjusted separately for each dry particle size. Figures 13 and 14 show the range of crystal interfacial tensions and disjoining pressures used in the calculations.

The magnitude and range of the disjoining pressure determine the steepness of the deliquescence curve: the higher the pressure, the more gradual the dissolution of the crystal becomes. On the other hand, if $\Pi(r, R)$ is set to zero, only the vertical stepwise transition can be found. Note that it would have been possible to fit all of the curves shown in Figures 8−12 using the same functional form for the disjoining pressure. This could have been carried out using a function that follows the 4 and 5 nm curves in Figure 14 at thin film values and approaches the 25 nm values when the film becomes thicker. However, using such a function leads to poorer agreement with the measured values, i.e., a too gentle departure of the 25 and 15 nm curves (Figures 8 and 9) from the dry particle value and a too gentle approach of the 7.5, 5, and 4 nm curves toward the fully dissolved droplets (Figures 10−12).

Roughly speaking, changing the crystal interfacial tension value causes the deliquescence curves to move along the RH scale (increased tension shifts the curve to lower RH). However, it would be too simplistic to say that the disjoining pressure only affects the slope of the deliquescence curve and the interfacial tension only affects its displacement. In fact, it is easy to choose a pair of functional forms for $\Pi(r, R)$ and $\sigma^{\beta\gamma}$ that result in an S-shaped deliquescence curve, which of course would be unphysical.

As can be seen from Figures 10−12, the deliquescence curves calculated for the 4−7.5 nm NaCl crystals are below the measured datapoints at relative humidities lower than about 75−80%. As with the more ideal systems of Figure 7, it would be possible to fit the crystal interfacial tension and the disjoining pressure so that the theory curves coincide with the measurements in this range. However, the good agreement seen at higher relative humidities would then be spoiled. Interestingly, conventional adsorption isotherms can reproduce the measurement data to relative humidities of about 70−75% but not at higher RHs (S. Romakkaniemi et al., manuscript in preparation).

It is rather easy to figure out a number of possible reasons for the somewhat disappointing fact that we have had to resort to nonunique functions for $\Pi(r, R)$ and $\sigma^{\beta\gamma}$ in reproducing the experimental results. These include the following:

(1) The exponential dependence of $\Pi(r, R)$ on film thickness may be incorrect when $h < l_1$ (see Churaev[23]).

(2) The interfacial tension $\sigma^{\beta\gamma}$ may depend on liquid composition.

(3) When the film is very thin, the underlying crystal may affect the structure of the liquid and thereby also the activities of water and NaCl.

(4) Also, the liquid−vapor surface tension may be affected when the film is thin.

(5) The problems in matching the theory with the experiment may be partly accounted for by the fact that the above-developed theory is purely thermodynamic, whereas the real evolution of particles during deliquescence is determined not only by the thermodynamics but also by the kinetics of the process.

(6) Finally, one must bear in mind the simpleminded thermodynamic treatment that we have used and especially the exclusion of surface excesses that would not only allow the interfacial tension to depend on composition but would surely affect the definition of particle radius (i.e., of dividing surface).

5. Concluding Remarks

We have developed a theory for the deliquescence of soluble crystals, as a function of the degree of saturation of the solvent vapor. The theory considers interfacial effects and is therefore applicable, in principle, to very small crystals (e.g., to crystals of nanometer size). The goal has been limited to the reproduction of only the qualitative features of the first experimental measurements on the deliquescence of such small crystals. Therefore, our thermodynamic theory has been simple minded and at the level of the "capillarity approximation" frequently used in nucleation theory. For example, we have not allowed surface excesses (interfacial adsorption), clearly defined Gibbs dividing surfaces, curvature effects, and many other refinements (e.g., nonspherical crystals) that should enter a rigorous theory.

Despite this, we have been able to verify several of the qualitative features of the experiments. However, the experimental feature that most stubbornly escapes us, even with respect to qualitative behavior, concerns what can be called "nonprompt" deliquescence. Prompt deliquescence is a phenomenon in which there is a discontinuous transition from an undeliquesced or partially deliquesced state to a fully deliquesced state at some critical level of vapor saturation. Nonprompt deliques-

cence involves a continuous dissolution of a core crystal as a function of vapor saturation and implies that a core crystal can coexist in equilibrium with a film of solution throughout a continuum of states leading from the undeliquesced to the fully deliquesced system. Unless we introduce unphysical behaviors of thermodynamic parameters such as interfacial tension and disjoining pressure, we are unable to predict such continuous phase coexistence. Clearly, something is missing, and a more sophisticated theory will be necessary before all of the qualitative features of measurement can be reproduced. Furthermore, there are now experiments[12,13c] with micron sized crystals that exhibit nonprompt deliquescence.

Together with the difficulty encountered in the development of a thermodynamic theory that allows coexistence of a partially dissolved core and a film of solution, this suggests that either there is still some surface thermodynamic feature missing from our theory or some bulk phenomenon takes place in the experiments that is difficult to account for, as is most likely the case with ammonium sulfate.[12,13c] The continuous (nonsharp) deliquescence in real systems may be due, for instance, to a difficultly controllable experimental variable such as the initial state of the core crystal. At the same time, our theory, in its present state, suggests that the equilibrium coexistence of core and solution is not possible in the deliquescence process. The systems that we have addressed are of atmospheric importance, e.g., $(NH_4)_2SO_4-H_2O$ and $NaCl-H_2O$. Among the new ideas that we have combined with the capillarity approximation is the concept of disjoining pressure that must be introduced in the treatment of very thin films. In focusing on the barrier to deliquescence, we have provided examples of free energy surfaces associated with the phenomenon. These landscapes allow insight into the paths that deliquescence processes can follow. In this connection, we have defined two distinct types of deliquescence. These are "activate deliquescence" and "nucleate deliquescence", processes that occur respectively in connection with barrierless deliquescence and deliquescence that does involve a free energy barrier.

Acknowledgment. The work was supported by NSF grant CHE0076384. A.L. acknowledges financial support from the Academy of Finland (project 50623).

Appendix: Derivation of eq 7

For future use we note, in the absence of surface adsorption, the geometric relations

$$R = [3(\nu_1 v_1 + \nu_2 v_2 + (\nu^{\gamma}{}_{20} - \nu_2)v^{\gamma}{}_2)/4\pi]^{1/3} \quad \text{(A1)}$$

$$r = [3(\nu^{\gamma}{}_{20} - \nu_2)v_2{}^{\gamma}/4\pi]^{1/3},\ r_0 = (3\nu^{\gamma}{}_{20}v_2{}^{\gamma}/4\pi)^{1/3} \quad \text{(A2)}$$

In the assumed absence of adsorption (no surface active components), the Gibbs adsorption equation[16,17] requires surface tensions to be independent of composition, so that the various defined σ's may be regarded as independent of ν_1 and ν_2. Of course, in the real system, there will be some adsorption and some dependence of surface tension on composition, but in the capillarity approximation to which we have appealed, we have assumed adsorption to be small enough to be approximated by zero. The omission of surface adsorption in the capillarity model was first noted by Renninger et al.[30] and Wilemski,[31] who modified the model to include surface accumulation. However, in the level of approximation adopted in this paper, we neglect such improvements.

Still another consequence of the neglect of adsorption is the applicability of the Gibbs−Duhem equation

$$\nu_1\, \mathrm{d}\mu^{\alpha}{}_1 + \nu_2\, \mathrm{d}\mu^{\alpha}{}_2 - (\nu_1 v_1 + \nu_2 v_2)\, \mathrm{d}P^{\alpha} = 0 \quad \text{(A3)}$$

to the film phase.

Equation 2 may be alternatively written as

$$\Delta G = \nu_1[\mu^{\alpha}{}_1(P^{\alpha},\chi^{\alpha}) - (P^{\alpha} - P)v_1 - \mu^{\beta}{}_1(P)] + \nu_2[\mu^{\alpha}{}_2(P^{\alpha},\chi^{\alpha}) - (P^{\alpha} - P)v_2 - \mu^{\gamma}{}_2(P^{\gamma}) + (P^{\gamma} - P)v^{\gamma}{}_2] + \sigma^{\alpha\beta}S^{\alpha\beta} + \sigma^{\alpha\gamma}S^{\alpha\gamma} - \sigma^{\gamma\beta}S^{\gamma\beta} \quad \text{(A4)}$$

It is clear from this equation together with eqs 4−6, A1, and A2 that ΔG depends at constant T and P only on ν_1 and ν_2. Now we take the partial derivative of ΔG, in eq A4, with respect to ν_1 and make use of eq A3. The result is

$$\frac{\partial \Delta G}{\partial \nu_1} = \mu^{\alpha}{}_1(P^{\alpha},\chi^{\alpha}) - \mu^{\beta}{}_1(P) + (P - P^{\alpha})v_1 + \sigma^{\alpha\beta}\frac{\partial S^{\alpha\beta}}{\partial \nu_1} + \sigma^{\alpha\gamma}\frac{\partial S^{\alpha\gamma}}{\partial \nu_1} - \sigma^{\gamma\beta}\frac{\partial S^{\gamma\beta}}{\partial \nu_1} \quad \text{(A5)}$$

where, in accordance with the above capillarity approximation, we have assumed the surface tensions to be independent of ν_1. Also, it is clear that $S^{\alpha\gamma}$ and $S^{\gamma\beta}$ are, by definition, independent of ν_1, so that the last two derivatives in eq A5 must be zero. It can also be shown (see below) that

$$(P - P^{\alpha})v_1 + \sigma^{\alpha\beta}\partial S^{\alpha\beta}/\nu_1 = 0 \quad \text{(A6)}$$

so that eq A5 reduces to

$$\frac{\partial \Delta G}{\partial \nu_1} = \mu^{\alpha}{}_1(P^{\alpha},\chi^{\alpha}) - \mu^{\beta}{}_1(P) \quad \text{(A7)}$$

To prove eq A6, we note that with the aid of eq A1

$$S^{\alpha\beta} = 4\pi[3(\nu_1 v_1 + \nu_2 v_2 + (\nu^{\gamma}{}_{20} - \nu_2)v^{\gamma}{}_2)/4\pi]^{2/3} \quad \text{(A8)}$$

Then, substitution of eqs A1 and A8 into the last term on the left of eq A6 converts that equation into eq 4; that is, eq A6 is a valid equation.

An exactly similar process, beginning with eq A4, but differentiating with respect to ν_2, yields

$$\frac{\partial \Delta G}{\partial \nu_2} = \mu^{\alpha}{}_2(P^{\alpha},\chi^{\alpha}) - \mu^{\beta}{}_2(P) \quad \text{(A9)}$$

Equations A7 and A9 are central to the further development of this paper. Although above they are obtained for systems in which the film (phase α) is thick enough, one cannot doubt their validity even when h is small enough so that, in the real system, the nonuniform layers at the $\alpha\beta$ and $\alpha\gamma$ interfaces overlap: eqs A7 and A9 should hold, but ΔG in these equations is no longer given by eq A4. Because this is the case during the initial stages of film formation, we need to address this problem. We do so below by introducing, among other things, the concept of the "disjoining pressure".[15]

If the liquid film on the solid core is not thick, as at the initial stages of its formation, one cannot represent the surface free energy of the film as the sum $\sigma^{\alpha\beta}S^{\alpha\beta} + \sigma^{\alpha\gamma}S^{\alpha\gamma}$ (see, e.g., refs 4, 7, 15, and 32).

In this case, one must use another method for the determination of the free energy of the intermediate state formation

which might be called the "integration" method. It consists of finding the free energy of formation ΔG of the intermediate state by integrating its complete differential $d\Delta G$ along some arbitrary path C leading from the initial to the intermediate state. Thus

$$\Delta G = \int_C d\Delta G \tag{A10}$$

In the case where the droplet does not contain any surface active substances (so that ν_1 and ν_2 are indeed the total respective numbers of molecules in the film), the complete differential $d\Delta G$ can be written as

$$d\Delta G = \frac{\partial \Delta G}{\partial \nu_1} d\nu_1 + \frac{\partial \Delta G}{\partial \nu_2} d\nu_2 \tag{A11}$$

Then, using eqs A7 and A9, one has

$$\Delta G = \int_C [\mu^{\alpha}{}_1(P^{\alpha}) - \mu^{\beta}{}_1(P)]\, d\nu_1 + [\mu^{\alpha}{}_2(P^{\alpha}) - \mu^{\gamma}{}_2(P^{\gamma})]\, d\nu_2 \tag{A12}$$

Equation A12 was used by Kuni et al.[33] in studying unary condensation on soluble particles consisting of surface inactive species, and Gorbunov and Hamilton[34] applied it to water condensation on mixed particles, but they did not derive it in the above presented manner nor did they use it in the manner developed below. Taking account of surface forces and making use of eq. A12, Djikaev and Donaldson[4] obtained the free energy of binary droplet formation on an insoluble particle, whereas Gorbunov[35] derived and analyzed the free energy of formation of a droplet on a mixed particle in a multicomponent vapor mixture.

Denote by z the total number of ions into which one solute molecule dissociates in the solution, i.e., $z = z^- + z^+$, and introduce the variables χ and x as

$$\chi = \frac{\nu_2}{\nu_1 + z\nu_2}, \quad x = \frac{\nu_2}{\nu_1 + \nu_2}$$

Clearly, x represents the nominal mole fraction of solute molecules in the solution (film), whereas the product $z\chi$ represents the total mole fraction of ions in the film. From now on, the composition of the film will be characterized by the variable χ. Assuming, as is usually done,[16,17] that the solid core and the liquid film are incompressible, the chemical potentials $\mu^{\alpha}{}_i(P^{\alpha},\chi)$ ($i = 1$ and 2) and $\mu^{\gamma}{}_2(P^{\gamma})$ can be represented as

$$\mu^{\alpha}{}_1(P^{\alpha},\chi) = \mu^{\alpha}{}_{1\infty} + kT \ln(\chi_1 f_1) + v_1(P^{\alpha} - P), \qquad \mu^{\beta}{}_1 = \mu^{\beta}{}_{1\infty} + kT \ln \zeta \tag{A13}$$

$$\mu^{\alpha}{}_2(P^{\alpha},\chi) = \mu^{\alpha}{}_{2\infty} + kTz \ln(\chi_2 f_2/\chi^* f^*{}_2) + v_2(P^{\alpha} - P), \qquad \mu^{\gamma}{}_2(P^{\gamma}) = \mu^{\gamma}{}_{2\infty} + v^{\gamma}{}_2(P^{\gamma} - P) \tag{A14}$$

where $\mu^{\alpha}{}_{1\infty}$ is the chemical potential of component 1 as a pure bulk liquid in equilibrium with pure vapor whose chemical potential is $\mu^{\beta}{}_{1\infty}$ (all chemical potentials without arguments and subscript "∞" are to be interpreted as at the pressure P) and $\mu^{\alpha}{}_{2\infty}$ is the chemical potential of component 2 in its saturated liquid solution (component 1 being the solvent) in equilibrium with the bulk solid phase of component 2, whereas $\mu^{\gamma}{}_{2\infty}$ represents the chemical potential of component 2 in its bulk solid state at pressure P. Furthermore, $\chi_1 = 1 - z\chi$ and $f_1 \equiv f_1(\chi)$ are the mole fraction and activity coefficient of component 1 in phase α of composition χ, and $f_2 \equiv f_2(\chi)$ is the mean ionic activity coefficient of component 2 in a liquid solution of composition χ. The asterisk indicates quantities associated with the saturated bulk solution. Clearly, χ^* is related to the nominal solubility of the solute (component 2) in the given solvent (component 1) by the relation

$$\chi^* = \frac{x^*}{1 + (z-1)x^*}$$

Finally, ζ is the saturation ratio of the vapor.

As is usually done,[4,16,33] in the RHS of the leftmost equality in eq A13, we neglect the difference $P - P_\infty$ in comparison to the pressure within the film, with P_∞ being the equilibrium vapor pressure at given temperature. (Note that, as pointed out by Kuni et al.,[33] this term may not be negligible for very large drops at very high pressures of an inert gas.)

According to Derjagin et al.,[15] the pressure within the film, P^{α}, is determined not only by the external (vapor) and capillary pressures but also by the disjoining pressure, so that

$$P^{\alpha} = P + \frac{2\sigma^{\alpha\beta}}{R} - \Pi \tag{A15}$$

where $\Pi \equiv \Pi(\chi, h)$ is the disjoining pressure within the film of composition χ and thickness $h = R - r$ (see also ref 4). For the pressure within the solid core, P^{γ}, we thus have

$$P^{\gamma} = P^{\alpha} + \frac{2\sigma^{\alpha\gamma}}{r} = P + \frac{2\sigma^{\alpha\beta}}{R} - \Pi + \frac{2\sigma^{\alpha\gamma}}{r} \tag{A16}$$

It should be noted that the concept of the disjoining pressure requires that at least one monolayer of *solution* should be formed on the solid core. As observed by Dai et al.,[36] the adsorption of water molecules onto hygroscopic surfaces occurs primarily at step edges or surface defects that have higher surface energy and are therefore more likely to be the adsorption sites. As suggested by these authors, hydration of surface ions at such sites weakens the ionic bond strength to the point where ions become mobile. Thus, water adsorbed on the ionic crystal surface solvates and detaches ions from the lattice, presumably starting at adsorption sites. For this reason, our theory assumes the existence of at least one monolayer of solution rather than a monolayer of water on the core and describes the evolution of drops with radii $R > R_{\min}$, where $R_{\min}$, the lower limit of applicability of the theory, is

$$R_{\min} = \left[r^3{}_0 + \frac{3\nu^*{}_1}{4\pi}\left(v_1 + \Delta v_2 \frac{x^*{}_0}{1 - x^*{}_0} \right) \right]^{1/3} \tag{A17}$$

Here $x^*{}_0$ is the nominal solubility of the initial, dry particle, i.e., the mole fraction of solute molecules in the solution saturated with respect to the particle (x_0^* depends on r_0, of course), and $\nu^*{}_1$ is the solution of the equation

$$\left[r^3{}_0 + \frac{3\nu^*{}_1}{4\pi}\left(v_1 + \Delta v_2 \frac{x^*{}_0}{1 - x^*{}_0} \right) \right]^{1/3} - \left[r^3{}_0 - \frac{3v^{\gamma}{}_2}{4\pi} \frac{x^*{}_0}{1 - x^*{}_0} \nu^*{}_2 \right]^{1/3} = 2\left[\frac{3(v_1(1 - x^*{}_0) + v_2 x^*{}_0)}{4\pi} \right]^{1/3}$$

(the RHS of this equation represents the thickness of a monolayer of solution of composition $x^*{}_0$).

Numerical calculations, based on reasonable assumed values of partial molecular volumes, show that $R_{\min}/r_0 \simeq 1.001$ for $r_0 = 15$ nm, $R_{\min}/r_0 \simeq 1.005$ for $r_0 = 10$ nm, and $R_{\min}/r_0 \simeq 1.04$

for $r_0 = 5$ nm. Note that these evaluations use the solubility of the bulk solid phase. The solubility of the particles increases with decreasing particle radius, but if this were taken into account, even lower values would be obtained for the lower limit R_{min} (which would mean a wider range of R), especially for small r_0.

By definition, $\mu^{\beta}{}_{1\infty} = \mu^{\alpha}{}_{1\infty}$ and $\mu^{\gamma}{}_{2\infty} = \mu^{\alpha}{}_{2\infty}$. Then substituting eqs A13 and A14 into eq A12, using eqs A15 and A16, and integrating along the path $\chi = \text{const}$ from the point ($\nu_1 = 0$ and $\nu_2 = 0$) to some arbitrary point (ν_1,ν_2), one obtains for ΔG expressed in units kT

$$\Delta G = -\nu_1 \ln\left[\frac{\zeta}{(1 - z\chi)f_1}\right] - \nu_2 z \ln\left[\frac{\chi^* f^*{}_2}{\chi f_2}\right] + \frac{1}{kT}(\sigma^{\alpha\beta}S^{\alpha\beta} + \sigma^{\alpha\gamma}S^{\alpha\gamma} - \sigma^{\gamma\beta}S^{\gamma\beta}) - \frac{v_1}{kT}\int_0^{\nu_1} \Pi(\chi, h)\, d\nu_1|_{\chi=\text{const}} - \frac{\Delta v_2}{kT}\int_0^{\nu_2} \Pi(\chi, h)\, d\nu_2|_{\chi=\text{const}} \quad \text{(A18)}$$

where we used Young's relation[16] $\sigma^{\alpha\beta} + \sigma^{\alpha\gamma} = \sigma^{\gamma\beta}$, assuming that the soluble particle is completely wettable (contact angle = 0). It is easy to show that if Π is equal to zero in this equation the result is eq 2, so that the two equations differ only by the work associated with the disjoining pressure.

Equation A18 provides the free energy of formation of a droplet on a soluble particle at partial dissolution. This expression takes account of the fact that at the early stages of the formation of a liquid film on the particle (and during the concomitant dissolution of the particle itself) the film is thin, and hence, the free energy barrier is lowered by the disjoining pressure within the film. By contrast to the capillary pressure, the disjoining pressure within a thin film on a lyophilic surface lowers the chemical potential of the condensate in the film and therefore makes it easier for condensate molecules to pass from vapor to film. The last terms on the right of eq A18 represent the contribution of the disjoining pressure Π to the free energy ΔG of the droplet (measured from its value for the dry nucleus). In closing this section, we remark that evaluating ΔG by integrating along the path $\chi = \text{const}$ involves the implicit assumption that the path represents a reversible process and that the same value ΔG would be obtained in an integration along any alternate path. The capillarity approximation does not guarantee this, so that eq A18 must be regarded, at best, as a valid approximation.

References and Notes

(1) Köhler, H. *Geofys. Pub. Krestiana* **1921**, *1*, 1.
(2) Köhler, H. *Geofys. Pub. Krestiana* **1922**, *2*, 6.
(3) Köhler, H. *Trans. Faraday Soc.* **1936**, *32*, 1152.
(4) Djikaev, Y. S.; Donaldson, D. J. *J. Geophys. Res. D* **1999**, *104*, 14283.
(5) Djikaev, Y. S.; Donaldson, D. J. *J. Chem. Phys.* **2000**, *113*, 6822.
(6) Kuni, F. M.; Shchekin, A. K.; Rusanov, A. I. *Colloid J. Russ. Acad. Sci.* **1993**, *55* (5), 686.
(7) Shchekin, A. K.; Rusanov, A. I.; Kuni, F. M. *Colloid J. Russ. Acad. Sci.* **1993**, *55* (5), 776.
(8) Mirabel, P.; Reiss, H.; Bowles, R. *J. Chem. Phys.* **2000**, *113*, 8194.
(9) Mirabel, P.; Reiss, H.; Bowles, R. *J. Chem. Phys.* **2000**, *113*, 8200.
(10) Lothe, J.; Pound, G. M. J. In *Nucleation*; Zettlemoyer, A. C., Ed.; Marcel-Dekker: New York, 1969.
(11) Tang, I. N.; Munkelwitz, H. R.; Wang, N. *J. Colloid Interface Sci.* **1986**, *114*, 409.
(12) Tang, I. N.; Munkelwitz, H. R. *Atmos. Environ.* **1993**, *27A*, 467; *J. Geophys. Res.* **1994**, *99*, 18801.
(13) (a) McMurry, P.; Stolzenburg, M. R. *Atmos. Environ.* **1989**, *23*, 497. (b) Svenningsson, I. B. *Hygroscopic growth of atmospheric aerosol particles and its relation to nucleation scavenging in clouds*, Ph.D. Thesis, Department of Nuclear Physics, University of Lund, Sweden, 1997. (c) Richardson, C. B.; Spann, J. F. *J. Aerosol Sci.* **1984**, *15*, 563.
(14) Hämeri, K.; Väkevä, M.; Hanssen, H.-C.; Laaksonen, A. *J. Geophys. Res.* **2000**, *105*, 22231.
(15) Derjaguin, B. V.; Churaev, N. V.; Muller, V. M. *Surface Forces*; Consult. Bur.: New York, 1987.
(16) Defay, R.; Prigogine, I.; Bellemans, A.; Everett, D. H. *Surface Tension and Adsorption*; John Wiley: New York, 1966.
(17) Debenedetti, P. G.; Reiss, H. *J. Chem. Phys.* **1998**, *108*, 5498.
(18) Debenedetti, P. G.; Reiss, H. *J. Chem. Phys.* **1999**, *111*, 3771.
(19) Nishioka, K.; Kusaka, I. *J. Chem. Phys.* **1992**, *96*, 5370.
(20) Hämeri, K.; Laaksonen, A.; Väkevä, M. *J. Geophys. Res.* **2001**, submitted.
(21) Reiss, H. *J. Chem. Phys.* **1950**, *18*, 840.
(22) Reiss, H. *Methods of Thermodynamics*; Dover: New York, 1996.
(23) Churaev, N. V. *Colloid J. USSR* **1984**, *46*(2), 262.
(24) Shugard, W. J.; Heist, R. H.; Reiss, H. *J. Chem. Phys.* **1974**, *61*, 5298.
(25) McGraw, R. *J. Chem. Phys.* **1995**, *102*, 2098.
(26) Pruppacher, H. R.; Klett, J. D. *Microphysics of Clouds and Precipitation*; Kluwer Academic Publishers: Dordrecht, The Netherlands, 1997.
(27) *CRC Handbook of Chemistry and Physics*, 76th ed.; CRC Press: New York, 1995.
(28) Bromley, L. A. *AIChE J.* **1973**, *19*, 313.
(29) Rowlinson, J. S.; Widom, B. *Molecular Theory of Capillarity*; Oxford University Press: New York, 1982.
(30) Renninger, R. G.; Hiller, F. C.; Bone, R. C. *J. Chem. Phys.* **1981**, *75*, 1584.
(31) Wilemski, G. *J. Chem. Phys.* **1984**, *80*, 1370.
(32) Rusanov, A. I.; Kuni, F. M. *Dokl. Phys. Chem.* **1991**, *318* (6), 467; *Colloids Surf.* **1991**, *61*, 349.
(33) Kuni, F. M.; Shchekin, A. K.; Rusanov, A. I. *Colloid J. Russ. Acad. Sci.* **1993**, *55* (2), 174.
(34) Gorbunov, B.; Hamilton, R. *J. Aerosol Sci.* **1997**, *28*, 239.
(35) Gorbunov, B. *J. Chem. Phys.* **1999**, *110*, 10035.
(36) Dai, Q.; Hu, J.; Salmeron, M. *J. Phys. Chem. B* **1997**, *101*, 1994.